

Reconstruction of 4D–CT data sets acquired during free breathing for the analysis of respiratory motion

Jan Ehrhardt^a, Rene Werner^a, Thorsten Frenzel^b, Dennis Säring^a, Wei Lu^c, Daniel Low^c and Heinz Handels^a

^aDepartment of Medical Informatics, University Medical Center Hamburg-Eppendorf, Germany

^bHermann Holthusen Institute of Radiotherapy, AK St. Georg, Hamburg, Germany

^cDepartment of Radiation Therapy, Washington University School of Medicine, St. Louis, USA.

ABSTRACT

Respiratory motion is a significant source of error in radiotherapy treatment planning. 4D–CT data sets can be useful to measure the impact of organ motion caused by breathing. But modern CT scanners can only scan a limited region of the body simultaneously and patients have to be scanned in segments consisting of multiple slices. For studying free breathing motion multislice CT scans can be collected simultaneously with digital spirometry over several breathing cycles. The 4D data set is assembled by sorting the free breathing multislice CT scans according to the couch position and the tidal volume. But artifacts can occur because there are no data segments for exactly the same tidal volume and all couch positions.

We present an optical flow based method for the reconstruction of 4D–CT data sets from multislice CT scans, which are collected simultaneously with digital spirometry. The optical flow between the scans is estimated by a non-linear registration method. The calculated velocity field is used to reconstruct a 4D–CT data set by interpolating data at user-defined tidal volumes. By this technique, artifacts can be reduced significantly. The reconstructed 4D–CT data sets are used for studying inner organ motion during the respiratory cycle.

The procedures described were applied to reconstruct 4D–CT data sets for four tumour patients who have been scanned during free breathing. The reconstructed 4D data sets were used to quantify organ displacements and to visualize the abdominothoracic organ motion.

Keywords: radiation therapy, 4D–CT, respiratory motion, optical flow, image registration

1. INTRODUCTION

Breathing motion is a significant source of error for the radiotherapy planning of the thorax and upper abdomen. In conventional conformal radiation therapy accounting for lung motion requires to enlarge the safety margins. As a consequence the volume of irradiated healthy tissue is increased substantially. Therefore, a main challenge in radiotherapy is to take breathing motion into account and to adapt the treatment according to this motion.

One approach is to use breath hold devices in order to immobilize the patient.¹ Another way to do is respiratory gating.² Gating techniques not directly compensate for breathing motion, instead the beam is switched off whenever the target is outside a predefined window. Often a combination of breath–hold techniques and respiratory gating is used. Such systems are actually in clinical use, for example *deep inspiration breath hold*³ or *active breath control*.⁴ Breath-hold techniques have the potential to reduce the effects of breathing motion, however, they are limited in practice by the fact that many patients cannot tolerate holding their breath. Furthermore, gating techniques are increasing the expense of time for the patient and physician significantly.⁵

The intention of 4D or real–time radiation therapy is to adapt the dose distribution to the organ motion during the respiratory cycle. Some attempts to explicitly account for free breathing motion are underway.^{5–7}

Further author information: (Send correspondence to J. Ehrhardt)

J. Ehrhardt: E-mail: j.ehrhardt@uke.uni-hamburg.de, Telephone: +49 40 42803 9934

but suffer from little existing knowledge regarding the spatiotemporal behavior of anatomical and pathological structures involved.

While, first approaches exist to solve the technical problems arising for motion adaptive radiation therapy, an accurate non-invasive tracking method for following the tumor motion is still needed. So in Schweikard et al. (2000)⁶ a robot arm is used to move the therapeutic beam generator and the dynamic adaptation of the shape of the dose distribution can be solved by multileaf collimators.⁵ But, a reliable biometric parameter correlated with breathing motion and an accurate spatiotemporal model of the respiratory motion is necessary to predict the target position.

4D-CT imaging can be used for the development of a model of free breathing motion and the identification of reliable biometrical parameters that could be applied to radiotherapy planning. Some approaches for the acquisition of 4D-CT data sets during free breathing were developed in the last years. Vedam et al. (2004)⁸ used a single slice spiral CT in combination with an external respiratory signal (an infrared-based motion tracking system) to generate a 4D-CT data set by sorting the acquired images according to predefined respiratory phases. In other applications a multislice CT scanner is operated in cine mode to acquire 4D data.⁹⁻¹¹ The advantage of 4D-CT imaging with multislice CT over single slice spiral CT is the improved spatial and temporal resolution, while the acquisition time is only slightly longer.¹⁰

But, modern multislice CT scanners cannot scan a large region of interest simultaneously. For this reason the patients have to be scanned in segments consisting of multiple slices acquired during several periods of the breathing cycle. If the acquired CT scans can be associated with tidal volumes or other biometrical parameters related to the respiratory cycle, a reconstruction of a 4D-CT data set is possible.^{9,10} But free breathing causes the problem that there are no segments for exactly the same period of the breathing cycle for each couch position. So artifacts occur similar to motion artifacts in 3D-CT.

In order to reduce these artifacts in this paper an optical flow based method for the reconstruction of 4D-CT data sets acquired during free breathing is presented. A non-linear registration method was implemented to calculate the optical flow. Following, a 4D-CT data set was reconstructed by generating interpolated data sets at user-defined respiratory volumes. The goal of this project is to use the reconstructed 4D-CT data sets for the development of a model of free breathing motion. This model can be used to analyze the spatiotemporal behavior of anatomical structures during the respiratory cycle and to find reliable biometric parameters correlated to free-breathing motion.

2. METHODS AND MATERIALS

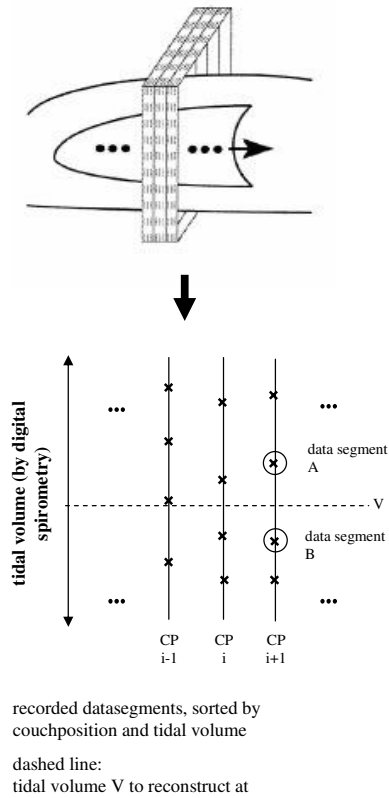
2.1. Data acquisition

A multislice CT scanner is operated in cine mode to acquire repeated scans per couch position over several free breathing cycles. Simultaneously the patient undergoes digital spirometry measurements. 15 scans were acquired at each couch position before the couch was moved to the adjacent position. This process was repeated until the entire thorax was scanned. For each patient, 16 – 19 couch positions were acquired scanned at 15 different times of the breathing cycle and each scan consists of 12 slices. Thus, each patient data set consists of 2880 to 3420 slices in total. To associate the CT scans with tidal volumes, simultaneous digital spirometry measurements were acquired. The patients were instructed to breath normally with the spirometer during the entire scanning sequence, which took approximately 10 min.

In a first approach the spirometry was used to generate a 4D image set by sorting free breathing multislice CT scans according to user-defined tidal volume bins. For a given tidal volume a 3D-CT data set was reconstructed by examining the spirometry record to determine which CT scan was acquired at a tidal volume closest to the desired volume at each couch position (see Low et al. (2003)⁹ for details). To prepare a time sequence of the motion (4D data set), the 3D data sets for a scale of tidal volumes were arranged in series.

Free breathing causes the problem that there are no acquired data segments for exactly the user-defined tidal volume. This induces artifacts similar to motion artifacts in 3D-CT. This is especially noticeable when viewing coronal reconstructions of the boundary between the diaphragm and the lung: the reconstructed diaphragm boundary shows an apparent and striking breakup (see fig. 2(left)).

Step 1: Data Acquisition



Step 2: Reconstruction

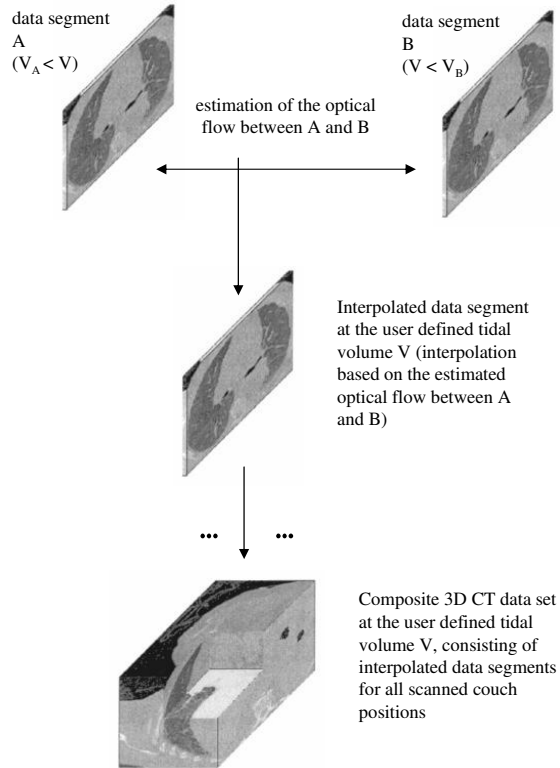


Figure 1. The process used to reconstruct a 4D-CT data set. The left section shows the CT scan acquisition using a multislice CT scanner. The scanner is operated in cine mode while the patient undergoes digital spirometry measurement. Thus, each acquired data segment is assigned to a couch position and a tidal volume (shown in the bottom left table). To reconstruct a 3D data set at a user-defined tidal volume V , for each couch position an interpolated data segment is generated. For a given couch position, the nearest data segments A and B with $V_A < V$ and $V_B > V$ are selected. The right side shows the interpolation process. First the optical flow between segment A and B is estimated. Following an interpolated data segment is generated. The last row of the right side shows the full 3D-CT scan created by stacking the interpolated scans from each couch position.

2.2. Optical flow based reconstruction of 4D-CT data sets

To avoid artifacts generated by missing CT scans for the desired volume an optical flow based reconstruction method was developed. In a first step, for each couch position the optical flow is determined between the scans measured with tidal volume closest to the selected one. Here, a non-linear registration algorithm computes a velocity field describing the deformation of corresponding features. Following, the calculated velocity field is used to generate an interpolated CT scan for the desired tidal volume (see fig. 1).

Computation of optical flow: Set $I_j(\mathbf{x}(V_i), V_i)$ for the CT scan at couch position j and tidal volume $V_i \in \{V_0 < V_1 < \dots < V_n\}$. Here, only volumes are regarded, which belong to the same breathing phase (inhalation or exhalation). The initial hypothesis of optical flow based methods is that pixel intensities of time varying image

regions remain constant.¹² In our case, the image function depends on the tidal volume V instead of the time:

$$\frac{dI(\mathbf{x}(V), V)}{dV} = 0. \quad (1)$$

From the optical flow equation (1) we obtain

$$\mathbf{v} = -\nabla I \frac{\partial V I}{\|\nabla I\|^2}, \quad (2)$$

where $\mathbf{v} = (\frac{\partial x}{\partial V}, \frac{\partial y}{\partial V}, \frac{\partial z}{\partial V})^T$ is the velocity field and ∇I the spatial image gradient. However, equation (2) is ill-posed and only the motion component in the direction of the local brightness gradient of the image intensity function may be estimated.¹² As a consequence, the flow velocity cannot be computed locally without introducing additional constraints. In our implementation the necessary regularization is done by Gaussian smoothing of the velocity field.

Given two images $I_j(\mathbf{x}(V_i), V_i)$ and $I_j(\mathbf{x}(V_{i+1}), V_{i+1})$, the velocity is computed by an iterative algorithm similar to *demons-based registration*¹³: first, the actual velocity field is estimated by eq. (3) and following a Gaussian smoothing of the velocity field is performed. The algorithm stops, if the deformed image $I_j(\mathbf{x} - \mathbf{v}(\mathbf{x}), V_{i+1})$ is most similar to $I_j(\mathbf{x}, V_i)$ or if a maximal number of iterations is reached. The derivatives in eq. (2) can be approximated by $\nabla I = (\nabla I_j(\mathbf{x}, V_i) + \nabla I_j(\mathbf{x}, V_{i+1}))/2$ and $\partial V I = I_j(\mathbf{x}, V_{i+1}) - I_j(\mathbf{x}, V_i)$, where $V_{i+1} - V_i = 1$ is assumed. For iteration $k + 1$ the velocity field is estimated by¹⁴:

$$\mathbf{v}_{k+1}(\mathbf{x}) = \mathbf{v}_k - \frac{2 (\nabla I_j(\mathbf{x}, V_i) + \nabla I_j(\mathbf{x} - \mathbf{v}_k(\mathbf{x}), V_{i+1})) (I_j(\mathbf{x} - \mathbf{v}_k(\mathbf{x}), V_{i+1}) - I_j(\mathbf{x}, V_i))}{\|\nabla I_j(\mathbf{x}, V_i) + \nabla I_j(\mathbf{x} - \mathbf{v}_k(\mathbf{x}), V_{i+1})\|^2} \quad (3)$$

The symmetric behavior of eq. (3) is advantageous for the interpolation step, but has the disadvantage that the gradient $\nabla I_j(\mathbf{x} - \mathbf{v}_k(\mathbf{x}), V_{i+1})$ has to be recomputed at each iteration, which is time-consuming.

Problems occur near segment borders. This is due to the existence of voxels that do not have corresponding voxels in the considered couch position, because some structures may change from one data segment into another segment during the respiratory cycle. To overcome this also CT scans at adjacent couch positions are taken into account for the registration process. To calculate the velocity field between $I_j(\mathbf{x}, V_i)$ and $I_j(\mathbf{x}, V_{i+1})$ two data volumes are assembled consisting of $I_{j-1}(\mathbf{x}, V'_i)$, $I_j(\mathbf{x}, V_i)$ and $I_{j+1}(\mathbf{x}, V'_i)$ and $I_{j-1}(\mathbf{x}, V'_{i+1})$, $I_j(\mathbf{x}, V_{i+1})$ and $I_{j+1}(\mathbf{x}, V'_{i+1})$ respectively. V'_i and V'_{i+1} are the nearest available tidal volumes at couch positions $j - 1$ or $j + 1$.

Optical flow based interpolation: Given two images for tidal volumes V_i and V_{i+1} and the velocity \mathbf{v} we want to interpolate the image $I_j(\mathbf{x}(V), V)$ at tidal volume $V \in [V_i, V_{i+1}]$. Regarding to the optical flow equation (1) we can write $I_j(\mathbf{x}(V), V) = I_j(\mathbf{x}(V) - \delta V \mathbf{v}, V_i)$. But in general the intensity conservation assumption might not be fulfilled and structures contained only in $I_j(\mathbf{x}(V_{i+1}), V_{i+1})$ are lost. Instead, we use a weighted average between the corresponding voxel intensities in $I_j(\mathbf{x}(V_i), V_i)$ and $I_j(\mathbf{x}(V_{i+1}), V_{i+1})$ ¹⁵:

$$I(\mathbf{x}(V), V) = (1 - \delta V) \cdot I_j(\mathbf{x}(V) - \delta V \mathbf{v}, V_i) + \delta V \cdot I_j(\mathbf{x}(V) - (1 - \delta V) \mathbf{v}^{-1}, V_{i+1}), \quad (4)$$

with a normalized interpolation factor $\delta V = \frac{V - V_i}{V_{i+1} - V_i}$. Generally, the inverse velocity field \mathbf{v}^{-1} can not be computed directly. In our interpolation scheme an iterative Newton-Raphson method is used to calculate the inverse velocity for each grid point.¹⁶ The optical flow-based registration matches corresponding features in the two images. In eq. (4) the interpolated grey value is the weighted average of the grey values of the corresponding features.

2.3. Analysis of respiratory motion

The resulting 4D-CT data set is used to analyze the respiratory motion. In a first step, the lung, the skin and the bronchial tree are segmented for any reconstructed tidal volume using region growing techniques and interactive correction. Surface models of the segmented organs are generated in order to enable the visualization of the 4D

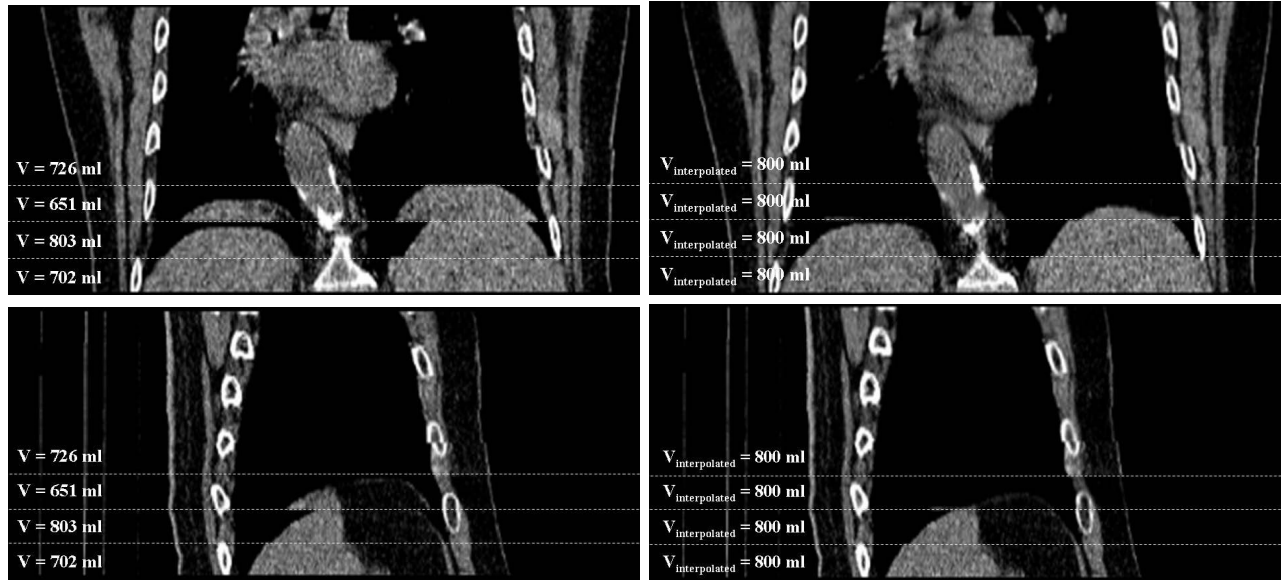


Figure 2. Coronal (top) and sagittal (bottom) section of a reconstructed 4D-CT data set at a tidal volume of 800 ml. Left: Artifacts at the diaphragm caused by free breathing motion. Right: Artifacts are reduced significantly after the optical flow based interpolation.

breathing motion. Anatomical landmarks, e.g. the trachial bifurcations, are determined interactively and the trajectories of the selected points are analyzed and visualized.

Furthermore, the segmented 4D data sets are used to calculate the optical flow of the organ surfaces. Therefore, a non-linear registration similar to the algorithm described in section 2.2 is performed. The resulting velocity fields are used to approximate the trajectories of points on the organ surface. So, the maximum displacement of any surface point can be calculated and regions with large respiratory motion are identified. Further on, the shape and deflection of different trajectories can be compared. By this technique, regions with highly correlated motion can be determined, for example regions of the skin which are correlated with the breathing motion of the diaphragm.

3. RESULTS

Four lung cancer patients were examined with a multislice CT scanner using the technique described in section 2.1. The resolution of the CT slices was between 0.78×0.78 and $0.94 \times 0.94 \text{ mm}^2$ and the spacing was 1.5 mm . For each patient a 4D-CT data sets were reconstructed, consisting of 10 3D-CT volumes. The 10 tidal volumes were selected in such a way that a complete breathing cycle was sampled temporally equidistantly. The relation between tidal volumes and time can be approximated by the following formula^{7,17}:

$$V(t) = V_{min} + V_{max} \cdot \sin^2 \left(\frac{\pi t}{\tau} \right), \quad (5)$$

where τ is the duration of a breathing cycle. The 4D-CT data sets were reconstructed 1) by sorting according to the selected tidal volume bins and 2) by optical flow based interpolation.

The first reconstruction method shows "steps" at the edges of neighbouring segments that were not scanned exactly at the same period of the breathing cycle (fig. 2(left)). With the optical flow based interpolation method described above the artifacts are reduced significantly on visual inspection (fig. 2(right)).

For a quantitative evaluation of the reconstruction methods, the average gray value difference between adjacent slices was calculated. Define MSD^{orig} the average squared gray value difference of the original CT scans

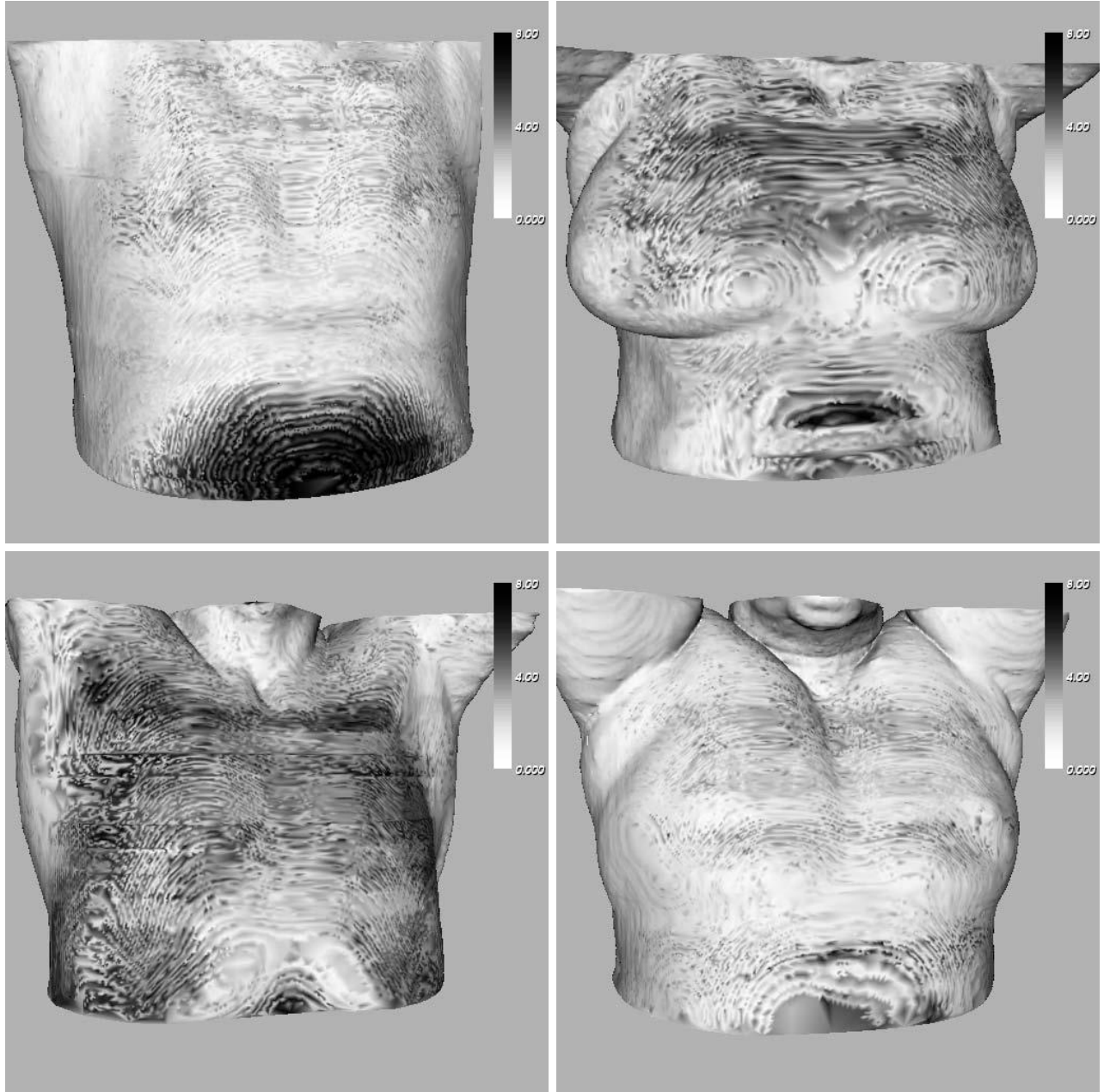


Figure 3. Visualization of the maximum displacement of the skin surface during the respiratory cycle of patient 1 (top left), patient 2 (top right), patient 3 (bottom left) and patient 4 (bottom right). Black surface points indicate a maximum displacement $\geq 5mm$ (scale: 0 – 8 mm).

I_j for each couch position:

$$MSD^{orig} = \frac{1}{N_j} \sum_{j=1}^{N_j} \frac{1}{11} \sum_{z=2}^{12} \frac{1}{|\Omega|} \sum_{(x,y) \in \Omega} (I_j(x,y,z-1) - I_j(x,y,z))^2. \quad (6)$$

N_j is the number of couch positions and each CT scan consists of 12 slices. For an interpolated 3D-CT data set, MSD^{int} designate the average slice changes at segment borders. Here, the average squared difference between

adjacent slices is calculated, which belong to different couch positions:

$$MSD^{int} = \frac{1}{\lfloor N_z/12 \rfloor} \sum_{\substack{z=2 \wedge \\ z \bmod 12=1}}^{N_z} \frac{1}{|\Omega|} \sum_{(x,y) \in \Omega} (I^{int}(x,y,z-1) - I^{int}(x,y,z))^2, \quad (7)$$

where I^{int} is the interpolated 3D data set for a selected tidal volume and N_z is the number of slices of the interpolated data set. Due to the problem, that there are no data segments for the desired tidal volume at each couch position, the slice changes at segment borders (eq. (7)) are higher than the slice changes inside the original data segment (eq. (6)). So, the difference $MSD^{int} - MSD^{orig}$ is a measure for the amount of artifacts at segment borders. To compare the optical flow based reconstruction method (*of*) and the reconstruction by sorting according to tidal volume bins (*sort*) the quotient of these differences was used:

$$r = \left| 1 - \frac{MSD^{of} - MSD^{orig}}{MSD^{sort} - MSD^{orig}} \right|. \quad (8)$$

For the four patient data sets the artifacts could be reduced by 31.8%, 29.9%, 30.7% and 41.6% (mean over ten tidal volumes).

The reconstructed 4D data sets were used to quantify organ displacements and to visualize the thoracic organ motion. In a first evaluation, anatomical landmarks, e.g. the tracheal bifurcation, tip of the lung, tip of the diaphragm, were selected manually and the displacement during the respiratory cycle was determined. The measured maximum displacements agree with standard values from other studies.¹⁸

Following, the determined velocity field was used to compute distances between organ surfaces at different respiratory states and to analyze the trajectories of landmarks and surface points. In fig. 3 the maximum displacement of all surface points of the skin during the respiratory cycle is visualized. The regions of maximum displacement differ between the patients. The clear differences between abdominal breathing (patient 1) and chest breathing (patient 2) can be recognized. The analysis of the reconstructed 4D-CT data sets is ongoing work and further results will be published elsewhere.

4. DISCUSSION AND CONCLUSION

Analysis, modelling and understanding of breathing motion is an essential condition for the proposed 4D radiotherapy, in which respiratory motion is explicitly accounted for in imaging, planning and delivery of radiotherapy. Multislice CT scanner can be used for generating 4D-CT data sets influenced by respiratory motion. In existing approaches, the 4D-CT data set is reconstructed by sorting the scans according to user-defined tidal volume bins.⁹⁻¹¹ Using this reconstruction method, artifacts occur similar to motion artifacts in 3D-CT imaging.

We have proposed a new optical flow based reconstruction method to generate 4D-CT data sets obtained from multislice CT scans acquired during free breathing. The visual and quantitative results indicate, that motion artifacts can be reduced significantly by this method. Thus, a precise modelling and analysis of the respiratory motion becomes possible. A drawback of our reconstruction method is the high computational cost of the optical flow based registration method. In the actual implementation the reconstruction of a 4D-CT data set consisting of $512 \times 512 \times 192 \times 10$ voxels requires more than 30 hours on a PC (2.2GHz AMD Opteron). Furthermore, a slight blurring of the interpolated data sets was observed. But, by visual inspection it is hard to distinguish original and interpolated slices.

First steps for an automated analysis of the reconstructed 4D-CT data sets were done. From segmented organ models trajectories of arbitrary points were calculated and regions with large respiratory motion can be identified automatically. Furthermore, the correlation between the motion of different regions can be calculated.

In a future implementation of the reconstruction method we will accelerate the registration process by using multi-resolution techniques and parallelization. Furthermore, the segmentation of 4D data sets using standard thresholding techniques combined with interactive correction turned out to be very time-consuming, because the number of organ contours increases by a factor of the number of desired tidal volumes. However, most of the segmentation process can be automated, and future work will include the development of improved segmentation

methods. The use of more than two consecutive slices for the calculation of the optical flow field may improve the registration accuracy and consequently the accuracy of the computed trajectories.¹⁵ But due to the increased requirements of memory and processing time a very efficient implementation of this registration algorithm is necessary.

Further works continues to analyze the intra- and inter-patient variation of the free breathing motion. A long-term goal of the work presented is to find correlations between the respiratory state and the motion of skin markers in order to reconstruct the abdominal organ motion from external, non-invasive tracking data.

REFERENCES

1. I. Lax, H. Blomgren, I. Naslund, and R. Svanstrom, "Stereotactic radiotherapy of malignancies in the abdomen. Methodological aspects," *Acta Oncol* **33**, pp. 677–683, 1994.
2. H. Kubo and B. Hill, "Respiration gated radiotherapy treatment: a technical study," *Phys Med Biol* **41**, 1996.
3. K. Rosenzweig, J. Hanley, D. Mah, *et al.*, "The deep inspiration breath-hold technique in the treatment of inoperable non-small-cell lung cancer," *Int J Radiat Oncol Biol Phys* **48**, pp. 81–87, 2000.
4. J. Wong, M. Sharpe, D. Jaffray, *et al.*, "The use of active breathing control (abc) to reduce margin for breathing motion," *Int J Radiat Oncol Biol Phys* **44**, pp. 911–919, 1999.
5. P. Keall, V. Kini, S. Vedam, and R. Mohan, "Motion adaptive x-ray therapy: a feasibility study," *Phys Med Biol* **46**, pp. 1–10, 2001.
6. A. Schweikard, G. Glosser, M. Bodduluri, *et al.*, "Robotic motion compensation for respiratory movement during radiosurgery," *Comput Aided Surg* **5**, pp. 263–77, 2000.
7. H. Shirato, Y. Seppenwoolde, K. Kitamura, *et al.*, "Intrafractional tumor motion: lung and liver," *Semin Radiat Oncol* **14**, pp. 10–18, 2004.
8. S. Vedam, P. Keall, A. Docef, *et al.*, "Predicting respiratory motion for four-dimensional radiotherapy," *Med Phys* **31**, pp. 2274–2283, 2004.
9. D.-A. Low, M. Nystrom, E. Kalinin, P. Parikh, J.-F. Dempsey, J.-D. Bradley, S. Mutic, S.-H. Wahab, T. Islam, G. Christensen, D.-G. Politte, and B.-R. Whiting, "A method for the reconstruction of four-dimensional synchronized CT scans acquired during free breathing," *Med.-Phys.* **30**(6), pp. 1254–63, 2003.
10. T. Pan, T.-Y. Lee, E. Rietzel, and G. Chen, "4D-CT imaging of a volume influenced by respiratory motion on multi-slice CT," *Med Phys* **31**, pp. 333–340, 2004.
11. W. Lu, P. Parikh, I. El Naqa, *et al.*, "Quantitation of the reconstruction quality of a four-dimensional computed tomography process for lung cancer patients," *Med Phys* **32**, pp. 890–901, 2005.
12. B. K. P. Horn and B. G. Schunck, "Determining optical flow.," *Artificial Intelligence* **17**, pp. 185–203, Aug. 1981.
13. J.-P. Thirion, "Image matching as a diffusion process: an analogy with maxwell's demons," *Medical Image Analysis* **2**(3), pp. 243–260, 1998.
14. J.-P. Thirion, "Fast non-rigid matching of 3D medical images," Tech. Rep. 2547, INRIA, 1995.
15. J. Ehrhardt, D. Säring, and H. Handels, "Interpolation of temporal image sequences by optical flow based registration," in *SPIE Medical Imaging 2006*, (San Diego), 2006. (accepted).
16. W. H. Press, S. A. Teukolsky, W. T. Vetterling, and B. P. Flannery, *Numerical recipes in C*, Cambridge University Press, 1992.
17. Y. Seppenwoolde, H. Shirato, K. Kitamura, *et al.*, "Precise and real-time measurement of 3d tumor motion in lung due to breathing and heartbeat, measured during radiotherapy," *Int J Radiat Oncol Biol Phys* **53**, pp. 822–834, 2002.
18. K. Langen and D. Jones, "Organ motion and its management," *Int J Radiat Oncol Biol Phys* **50**, pp. 265–278, 2001.